22. McGinley, C. *et al.* Evidence for surface reconstruction on InAs nanocrystals. *Phys. Rev. B* **65,** 245308 (2002).
23. Meulenberg, R. W. & Strouse, G. F. Vibrational analysis of nanocrystal CdSe surfaces: Evidence for surface reconstruction. *Abstr. Pap. Am. Chem. Soc.* **220,** 404-Phys (2000).
24. Hertl, W. Surface chemical properties of zinc sulfide. *Langmuir* **4,** 594–598 (1988).
25. Rockenburger, J. *et al.* The contributions of particle core and surface to strain, disorder and vibrations in thiolcapped CdTe nanocrystals. *J. Chem. Phys.* **108,** 7807–7815 (1998).
26. Head-Gordon, T. & Hura, G. Water structure from scattering experiments and simulation. *Chem. Rev.* **102,** 2651–2670 (2002).
27. Guinier, A. *X-Ray Diffraction in Crystals, Imperfect Crystals and Amorphous Bodies* (Freeman & Co., San Francisco, 1963).
28. Wright, K. & Jackson, R. A. Computer simulations of the structure and defect properties of zinc sulfide. *J. Mater. Chem.* **5,** 2037–2040 (1995).
29. Desgreniers, S., Beaulieu, L. & Leparge, I. Pressure-induced structural changes in ZnS. *Phys. Rev. B* **61,** 8726–8733 (2000).
30. de Leeuw, N. H. & Parker, S. C. Molecular-dynamics simulation of MgO surfaces in liquid water using a shell-model potential for water. *Phys. Rev. B* **58,** 13901–13908 (1998).
31. Berendsen, H. J. C., Grigera, J. R. & Straatsma, T. P. The missing term in effective pair potentials. *J. Phys. Chem.* **91,** 6269–6271 (1987).
32. Stillinger, F. H. & Rahman, A. Revised central force potentials for water. *J. Chem. Phys.* **68,** 666–670 (1978).
33. Harris, D. J., Brodholt, J. P., Harding, J. H. & Sherman, D. M. Molecular dynamics simulation of aqueous $ZnCl_2$ solutions. *Mol. Phys.* **99,** 825–833 (2001).
34. Stevens, J. E., Chaudhuri, R. K. & Freed, K. F. Global three-dimensional potential energy surfaces of H_2S from the *ab initio* effective valence shell Hamiltonian method. *J. Chem. Phys.* **105,** 8754–8768 (1996).

Supplementary Information accompanies the paper on **www.nature.com/nature**.

Acknowledgements We thank P. Alivisatos for access to equipment, and W. Smith, T. R. Forester and D. Fincham for providing MD codes. EXAFS data were acquired on the DCM beamline at the UW-Madison Synchrotron Radiation Center (SRC), and we thank A. Jürgensen. WAXS data were acquired on beamline 11-ID-C at the Advanced Photon Source (APS), and we thank Y. Ren and M. Beno. HRTEM was performed at the National Center for Electron Microscopy, Berkeley, California. We also thank J. Rustad and G. Waychunas for discussions. This work was supported by the US Department of Energy (DOE), the Lawrence Berkeley National Laboratory LDRD, and the US National Science Foundation (NSF). The SRC is supported by the Division of Materials Research of the US NSF. Use of the Advanced Photon Source is supported by the US DOE, Office of Science, Office of Basic Energy Sciences.

Competing interests statement The authors declare that they have no competing financial interests.

Correspondence and requests for materials should be addressed to J.F.B. (jill@eps.berkeley.edu).

Controlling molecular deposition and layer structure with supramolecular surface assemblies

James A. Theobald[1], Neil S. Oxtoby[2], Michael A. Phillips[1], Neil R. Champness[2] & Peter H. Beton[1]

[1]*School of Physics and Astronomy,* [2]*School of Chemistry, University of Nottingham, Nottingham NG7 2RD, UK*

Selective non-covalent interactions have been widely exploited in solution-based chemistry to direct the assembly of molecules into nanometre-sized functional structures such as capsules, switches and prototype machines[1–5]. More recently, the concepts of supramolecular organization have also been applied to two-dimensional assemblies on surfaces[6,7] stabilized by hydrogen bonding[8–14], dipolar coupling[15–17] or metal co-ordination[18]. Structures realized to date include isolated rows[8,13–15], clusters[9,10,18] and extended networks[10–12,17], as well as more complex multi-component arrangements[16]. Another approach to controlling surface structures uses adsorbed molecular monolayers to create preferential binding sites that accommodate individual target molecules[19,20]. Here we combine these approaches, by using hydrogen bonding to guide the assembly of two types of molecules into a two-dimensional open honeycomb network that then controls and templates new surface phases formed by subsequently deposited fullerene molecules. We find that the open network acts as a two-dimensional array of large pores of sufficient capacity to accommodate several large guest molecules, with the network itself also serving as a template for the formation of a fullerene layer.

We investigate an open honeycomb network formed when perylene tetra-carboxylic di-imide (PTCDI; Fig. 1a) is co-adsorbed with melamine (1,3,5-triazine-2,4,6-triamine; Fig. 1b) on a silver-terminated silicon surface. Melamine, which has a three-fold symmetry, forms the vertices of the network while the straight edges correspond to PTCDI. The network is stabilized by melamine–PTCDI hydrogen bonding. Melamine and PTCDI were chosen for this application because they are expected to exhibit much stronger hetero- as opposed to homo-molecular hydrogen bonding. As shown in Fig. 1, the compatibility of molecular geometries results in three hydrogen bonds per melamine–PTCDI pair, as compared

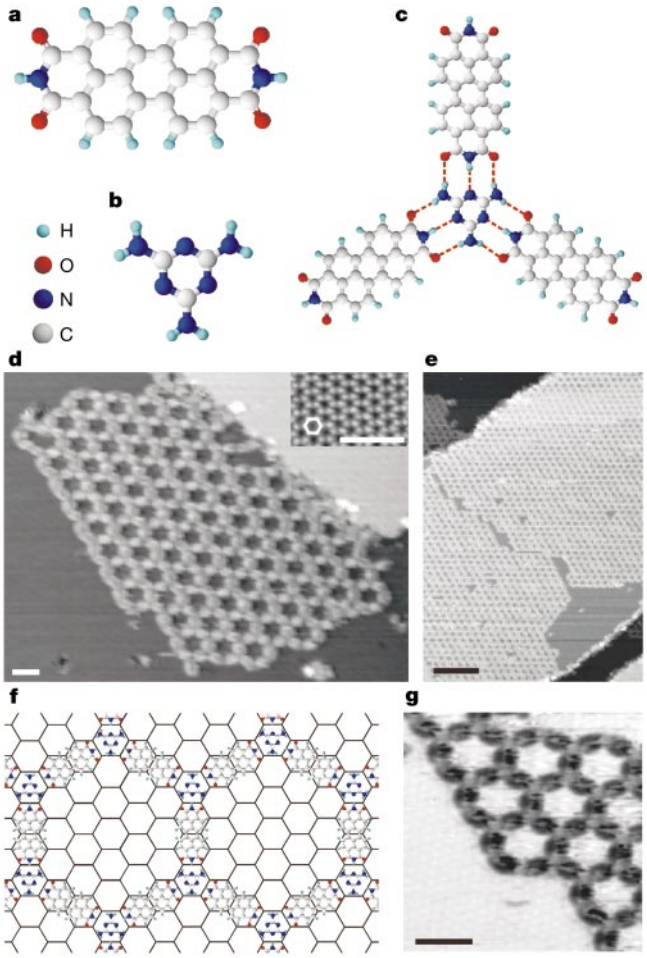

Figure 1 Self-assembly of a PTCDI–melamine supramolecular network. **a**, **b**, Chemical structure of PTCDI (**a**) and melamine (**b**). **c**, Schematic diagram of a PTCDI–melamine junction. Dotted lines represent the stabilizing hydrogen bonds between the molecules. **d**, STM image of a PTCDI–melamine network (sample voltage −2 V, tunnel current 0.1 nA). Inset, high-resolution view of the Ag/Si(111)-$\sqrt{3} \times \sqrt{3}$R30° substrate surface; the vertices and centres of hexagons correspond, respectively, to the bright (Ag trimers) and dark (Si trimers) topographic features in the STM image (surface lattice constant, $a_0 = 6.65$ Å; ref. 22). Scale bars, 3 nm. **e**, STM image of large-area network, with domains extending across terraces on the Ag/Si(111)-$\sqrt{3} \times \sqrt{3}$R30° surface (−2 V, 0.1 nA). Scale bar, 20 nm. **f**, Schematic diagram showing the registry of the network with the surface. **g**, Inverted contrast image (−2 V, 0.1 nA) of the network. Scale bar, 3 nm.

with just two for a PTCDI or melamine pair. The supramolecular synthon used in the melamine–PTCDI interaction has been shown to be very robust in solution-based supramolecular chemistry[21,22].

The network is prepared under ultra-high vacuum (UHV) conditions (base pressure $\sim 5 \times 10^{-11}$ torr). PTCDI and melamine were placed in effusion cells and sublimed (by heating to ~360 °C and ~100 °C, respectively) onto a Ag/Si(111)-$\sqrt{3} \times \sqrt{3}$R30° surface that had been prepared using standard procedures[23]. The choice of substrate was motivated by previous studies which showed that molecules such as fullerenes, phthalocyanines and napthalene tetracarboxylic di-imide (NTCDI, closely related to PTCDI)[13,23–26] diffuse freely on the Ag/Si(111)-$\sqrt{3} \times \sqrt{3}$R30° surface, and form islands in which the order is predominantly governed by intermolecular interactions. Images of the surface were acquired using a scanning tunnelling microscope (STM) housed within the UHV system and operating at room temperature. The Ag/Si(111)-$\sqrt{3} \times \sqrt{3}$R30° surface (Fig. 1d inset) has been studied extensively, and is described by the honeycomb-chain-trimer model in which each surface Si atom is bonded to one Ag atom[27,28]. To simplify the subsequent discussion, we represent this surface by a hexagonal network[25].

The first step in the formation of the network is deposition of 0.1–0.3 monolayers (ML) of PTCDI onto a surface held at room-temperature, after which close packed islands and short chains similar to those reported in previous studies of PTCDI and NTCDI[13,29] are observed. Melamine is then deposited while the sample is annealed at ~100 °C. STM images of the resulting molecular network are shown in Fig. 1. The network has principal axes at 30° to those of the Ag/Si(111)-$\sqrt{3} \times \sqrt{3}$R30° surface, and a lattice constant $3\sqrt{3}a_0 = 34.6$ Å. In images with inverted topographic contrast (Fig. 1g), the positions of the two molecules may be clearly discerned, with melamine and PTCDI forming respectively the vertices and edges of the network, which is stabilized by the hydrogen bonding illustrated in Fig. 1c. The maximum surface coverage of the network observed to date is 50% (sample shown in large-area STM image, Fig. 1e). The registry of the molecules with respect to the underlying surface has been determined, and is shown schematically in Fig. 1f. Numerical calculations (Austin method 1[30]) give the centre-to-centre spacing of a single PTCDI–melamine pair as 10.2 Å, close to the observed separation of $1.5a_0 = 9.98$ Å. Thus the calculated melamine–melamine separation has a near-commensurability with the surface lattice.

Annealing provides sufficient thermal energy for molecules to detach from PTCDI islands and diffuse across the surface. These PTCDI molecules interact with melamine to nucleate the hexagonal

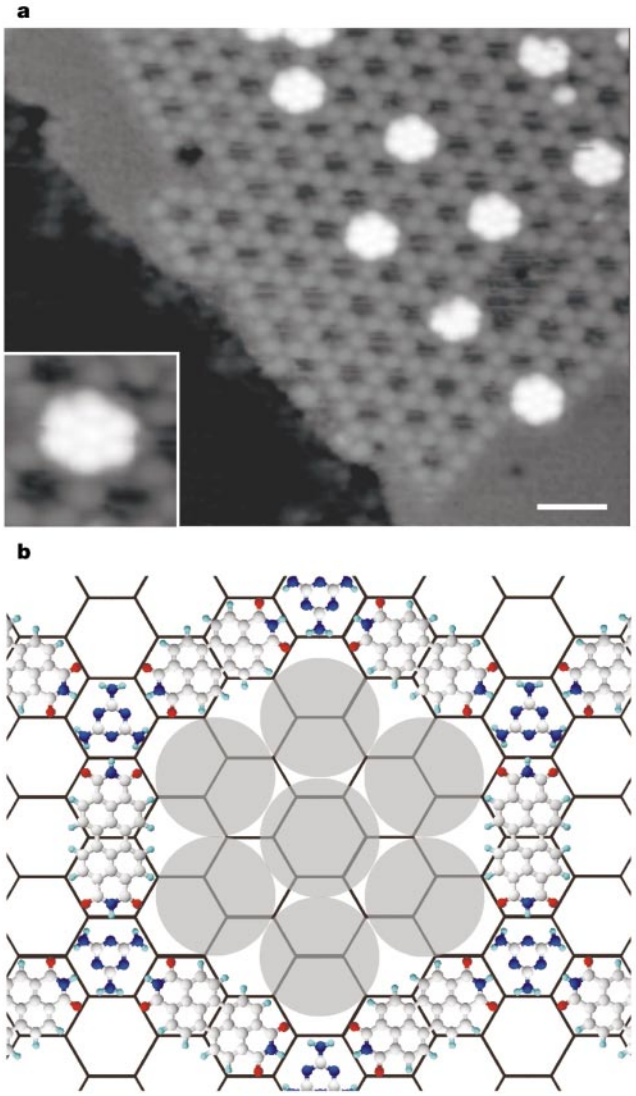

Figure 2 Images of C_{60} heptamers trapped within the 'nanoscale vessels'. **a**, STM image (−2 V, 0.1 nA) of C_{60} heptamers on a PTCDI–melamine network. Inset, high-resolution view showing an individual cluster. Scale bar, 5 nm. **b**, Schematic diagram of a C_{60} heptamer.

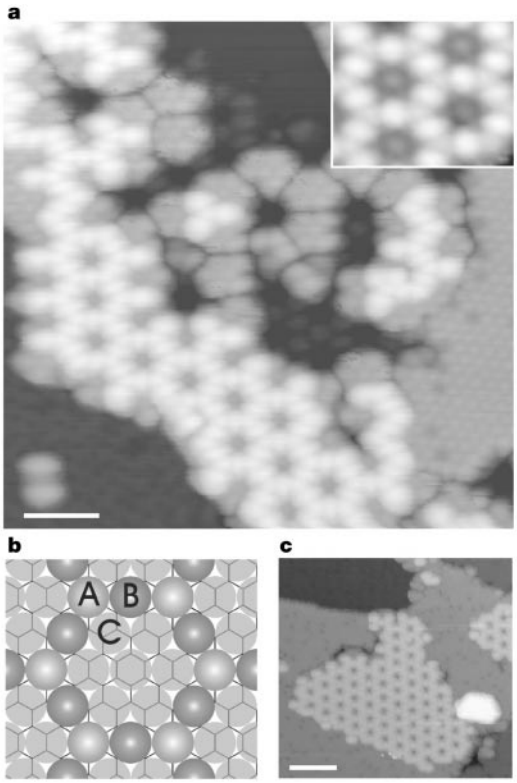

Figure 3 Images of the C_{60} honeycomb network. **a**, Image showing the PTCDI–melamine lattice, C_{60} heptamers and the raised C_{60} honeycomb network (−2 V, 0.1 nA). Scale bar, 5 nm. Inset, high-resolution view showing the C_{60} honeycomb network. **b**, Schematic diagram showing the registry of the raised C_{60} network with the surface. The hexagonal network of C_{60} molecules, marked A and B, sit directly above the melamine and PTCDI, respectively. These molecules are raised with respect to the heptamers by 2.1 and 2.8 Å, respectively. The elevation of molecules A and B results in an increase in their separation from molecules at the heptamer edge (marked C) to ~10.3 Å (assuming no lateral relaxation of the heptamer molecules — this cannot be resolved from STM images). **c**, Low defect termination of a PTCDI–melamine lattice with C_{60} (−2 V, 0.1 nA). Scale bar, 10 nm.

network, which then grows through further capture of diffusing molecules. If deposition of PTCDI is continued or restarted during formation of the network, the pores become 'filled' with other PTCDI molecules, presumably by their direct impinging on the pore area. The open network may only be formed from PTCDI molecules released from pre-formed islands and thus constrained to two-dimensional diffusion on the surface. The stepwise introduction of the two components is thus vital for the synthesis of the PTCDI–melamine network.

Hexagonal networks assembled from a single molecular species have been reported previously[10–12,17]. The open areas in such networks are small, comparable in size to that of a single molecular component of the supramolecular array[11]. In contrast, the incorporation of linear PTCDI edge molecules into a bimolecular assembly yields pores that are much larger than the constituent building blocks of the network and thus capable of serving as traps, or vessels, for the co-location of several large molecules. We demonstrate this potential by subliming C_{60} onto the hexagonal network. As shown in Fig. 2a, which shows an STM image acquired after deposition of 0.03 ML of C_{60}, heptameric C_{60} clusters with a compact hexagonal arrangement of the individual molecules form within the pores. Clusters formed in different pores are aligned, and are all oriented parallel to the principal axes of the Si(111) surface. The molecular arrangement of the heptamers has been deduced from STM images (Fig. 2b). Clusters of fewer molecules are also observed. For example, there are clusters of six molecules in Fig. 2a and clusters of 2–5 molecules have also been observed, while many pores remain empty for this coverage of C_{60}.

Previous studies of C_{60} on Ag/Si(111)-$\sqrt{3} \times \sqrt{3}$R30° observed extended monolayers and multilayer islands, but not isolated hexagonal heptameric clusters such as those in Fig. 2[25,26]. Moreover, whereas the most stable C_{60} islands on Ag/Si(111)-$\sqrt{3} \times \sqrt{3}$R30° were previously found to be hexagonally close-packed, their principal axes were misoriented with respect to the underlying surface[25,26] and the clusters were thus off-axis, unlike the on-axis heptamers observed here. These observations clearly indicate that the heptamers are stabilized by the PTCDI–melamine network.

The fraction of pores containing adsorbed molecules and stabilized heptameric clusters increases with increasing C_{60} coverage. In addition, we observe adsorption of C_{60} directly above the PTCDI and melamine molecules, thus reproducing the underlying hexagonal network. Figure 3a shows STM images of second-layer C_{60}, heptamers and the PTCDI–melamine network in close proximity. A further increase in C_{60} coverage results in a near-perfect termination of the second layer (see STM images in Fig. 3a, c). An array of C_{60} molecules sits directly above the melamine–PTCDI network (Fig. 3b), with the lateral positions within this array corresponding exactly to those of a hexagonally close-packed layer. The elevation of the hexagonal network's constituent molecules increases their separation from molecules at the heptamer edge, and this arrangement thus constitutes a new fullerene surface phase that is controlled and templated by the underlying hydrogen-bonded network.

Further deposition of C_{60}, up to a total of 3 ML, does not lead to the formation of additional fullerene layers on the hexagonal network. We attribute this observation to the termination layer (Fig. 3) lacking sites for the stable nucleation of additional layers. In particular, we find that the largest close-packed cluster that could form in a subsequent layer would contain only three molecules, rendering the cluster kinetically unstable at room temperature. Molecules incident on the hexagonal network diffuse to regions of the Ag/Si(111)-$\sqrt{3} \times \sqrt{3}$R30° surface that are not yet terminated, and where they are incorporated in close-packed fullerene islands that act as a sink for incident C_{60}. This suppression of nucleation, which is likely to depend on preparation conditions such as substrate temperature, accounts for the high degree of perfection of the termination observed in Fig. 3c.

Our results show that large pore areas can induce the co-location of several molecules in a 'nanoscale vessel'. Such pores might also prove useful in achieving the controlled co-location of a wider range of guest species, which could in turn lead to the promotion of local chemical interactions, controlled polymerization and the formation of complex supramolecular surface structures. □

Received 13 March; accepted 17 July 2003; doi:10.1038/nature01915.

1. Lehn, J. M. Toward complex matter: Supramolecular chemistry and self-organization. *Proc. Natl Acad. Sci. USA* **99,** 4763–4768 (2002).
2. Balzani, V., Credi, A., Raymo, F. M. & Stoddart, J. F. Artificial molecular machines. *Angew. Chem. Int. Edn Engl.* **39,** 3349–3391 (2000).
3. Reinhoudt, D. N. & Crego-Calama, M. Synthesis beyond the molecule. *Science* **295,** 2403–2407 (2002).
4. Fujita, M., Fujita, N., Ogura, K. & Yamaguchi, K. Spontaneous assembly of ten components into two interlocked, identical coordination cages. *Nature* **400,** 52–55 (1999).
5. Seeman, N. C. DNA in a material world. *Nature* **421,** 427–431 (2003).
6. Hecht, S. Welding, organizing, and planting organic molecules on substrate surfaces — Promising approaches towards nanoarchitectonics from the bottom up. *Angew. Chem. Int. Edn Engl.* **42,** 24–26 (2003).
7. De Feyter, S. & De Schryver, F. C. Two-dimensional supramolecular self-assembly probed by scanning tunnelling microscopy. *Chem. Soc. Rev.* **32,** 139–150 (2003).
8. Barth, J. V. *et al.* Building supramolecular nanostructures at surfaces by hydrogen bonding. *Angew. Chem. Int. Edn Engl.* **39,** 1230–1234 (2000).
9. Bohringer, M., Morgenstern, K., Schneider, W. D. & Berndt, R. Separation of a racemic mixture of two-dimensional molecular clusters by scanning tunneling microscopy. *Angew. Chem. Int. Edn Engl.* **38,** 821–823 (1999).
10. Furukawa, M., Tanaka, H. & Kawai, T. Formation mechanism of low-dimensional superstructure of adenine molecules and its control by chemical modification: A low-temperature scanning tunneling microscopy study. *Surf. Sci.* **445,** 1–10 (2000).
11. Griessl, S., Lackinger, M., Edelwirth, M., Hietschold, M. & Heckl, W. M. Self-assembled two-dimensional molecular host-guest architectures from trimesic acid. *Single Mol.* **3,** 25–31 (2002).
12. Dmitriev, A., Lin, N., Weckesser, J., Barth, J. V. & Kern, K. Supramolecular assemblies of trimesic acid on a Cu(100) surface. *J. Phys. Chem. B* **106,** 6907–6912 (2002).
13. Keeling, D. L. *et al.* Assembly and processing of hydrogen bond induced supramolecular nanostructures. *Nano Lett.* **3,** 9–12 (2003).
14. Chen, Q., Frankel, D. J. & Richardson, N. V. Self-assembly of adenine on Cu(110) surfaces. *Langmuir* **18,** 3219–3225 (2002).
15. Yokoyama, T., Yokoyama, S., Kamikado, T., Okuno, Y. & Mashiko, S. Selective assembly on a surface of supramolecular aggregates with controlled size and shape. *Nature* **413,** 619–621 (2001).
16. de Wild, M. *et al.* A novel route to molecular self-assembly: Self-intermixed monolayer phases. *ChemPhysChem* **3,** 881–885 (2002).
17. Berner, S. *et al.* Time evolution analysis of a 2D solid-gas equilibrium: A model system for molecular adsorption and diffusion. *Chem. Phys. Lett.* **348,** 175–181 (2001).
18. Lin, N., Dmitriev, A., Weckesser, J., Barth, J. V. & Kern, K. Real-time single-molecule imaging of the formation and dynamics of coordination compounds. *Angew. Chem. Int. Edn Engl.* **41,** 4779–4783 (2002).
19. Gimzewski, J. K., Jung, T. A., Cuberes, M. T. & Schlittler, R. R. Scanning tunneling microscopy of individual molecules: Beyond imaging. *Surf. Sci.* **386,** 101–114 (1997).
20. Cuberes, M. T., Schlittler, R. R. & Gimzewski, J. K. Room temperature supramolecular repositioning at molecular interfaces using a scanning tunneling microscope. *Surf. Sci.* **371,** L231–L234 (1997).
21. Paraschiv, V. *et al.* Molecular "chaperones" guide the spontaneous formation of a 15-component hydrogen-bonded assembly. *J. Am. Chem. Soc.* **124,** 7638–7639 (2002).
22. Prins, L. J., Reinhoudt, D. N. & Timmerman, P. Noncovalent synthesis using hydrogen bonding. *Angew. Chem. Int. Edn Engl.* **40,** 2383–2426 (2001).
23. Wan, K. J., Lin, X. F. & Nogami, J. Surface reconstructions in the Ag/Si(111) system. *Phys. Rev. B* **47,** 13700–13712 (1993).
24. Upward, M. D., Beton, P. H. & Moriarty, P. Adsorption of cobalt phthalocyanine on Ag terminated Si(111). *Surf. Sci.* **441,** 21–25 (1999).
25. Upward, M. D., Moriarty, P. & Beton, P. H. Double domain ordering and selective removal of C_{60} on Ag/Si(111)-$\sqrt{3} \times \sqrt{3}$R30°. *Phys. Rev. B* **56,** R1704–R1707 (1997).
26. Nakayama, T., Onoe, J., Takeuchi, K. & Aono, M. Weakly bound and strained C_{60} monolayer on the Si(111)-$\sqrt{3} \times \sqrt{3}$R30°-Ag substrate surface. *Phys. Rev. B* **59,** 12627–12631 (1999).
27. Takahashi, T., Nakatani, S., Okamoto, N., Ishikawa, T. & Kikuta, S. A Study of the Si(111)-$\sqrt{3} \times \sqrt{3}$-Ag surface by transmission-X-ray diffraction and X-ray-diffraction topography. *Surf. Sci.* **242,** 54–58 (1991).
28. Katayama, M., Williams, R. S., Kato, M., Nomura, E. & Aono, M. Structure analysis of the Si(111)-$\sqrt{3} \times \sqrt{3}$R30°-Ag Surface. *Phys. Rev. Lett.* **66,** 2762–2765 (1991).
29. Uder, B., Ludwig, C., Petersen, J., Gompf, B. & Eisenmenger, W. STM characterization of organic molecules on H-terminated Si(111). *Z. Phys. B* **97,** 389–390 (1995).
30. Dewar, M. J. S., Zoebisch, E. G., Healy, E. F. & Stewart, J. J. P. The development and use of quantum-mechanical molecular models, 76. AM1 — a new general-purpose quantum-mechanical molecular model. *J. Am. Chem. Soc.* **107,** 3902–3909 (1985).

Acknowledgements We thank P. Moriarty and J. O'Shea for discussions, and N. Besley and P. Gill for advice on numerical calculations. This work was supported by the UK Engineering and Physical Sciences Research Council.

Competing interests statement The authors declare that they have no competing financial interests.

Correspondence and requests for materials should be addressed to N.R.C. (Neil.Champness@nottingham.ac.uk) or P.H.B. (Peter.Beton@nottingham.ac.uk).